Halftone Type of Soft-proofing and Hard-proofing Applications for High-Fidelity Printing Systems Using Six and Seven Colorants

Mei-Chun Lo[1] and Chong-Zhi Guo[2]

Keywords: iccMAX, color management, profile, CMM, packaging

Abstract

As desktop color publishing systems become more ubiquitous, the technical community, therefore, is being driven by the high-end color market to develop new technologies of HDR imaging and Hi-Fi color printing process, to differentiate and add value to their product. The intent is, via the use of HDR contone image, to produce Hi-Fi halftone images of superior color with maximum isomerism, an increase of the attainable color gamut, and more tone and detail than those with traditional processes. Additionally, in the field of Graphic Arts, multiple-primary displays with high-definition or wide color-gamut are practically used as soft-proofing for desktop color publishing.

Therefore, as motivated by the idea to bridge the gap between high-dynamic-range (HDR) imaging and high-fidelity color reproduction in the high-end of Graphic Arts industry, the aim of this research has two tasks. Firstly, it's to derive an HDR contone to Hi-Fi halftone-conversion characterization model for both six-colorant CMYKOG and seven-colorant CMYKORG printing systems, via fitting spectral-reflectance approach. It is optimally revised and extended from a previous research. The supersets of CMYKOG and CMYKRGB were divided into three subsets and four subsets respectively. The superset of CMYKOG includes two five-colorant subsets of CMYKO and CMYKG, and one four-colorant subset of CMYK; whereas the CMYKRGB applies three five-colorant subsets of CMYKR, CMYKG and CMYKB, and one four-colorant subset of CMYK. The spectral printer characterization carries out a polynomial regression approach with singular value decomposition method (SVD). In total, 1617 and 1716 color patches are respectively used in test targets of four-colorant and five-colorant subsets for the printing

[1] Dept. of Information Management, Shih Hsin University, Taiwan, R.O.C.
[2] Dept. of Graphic Communications and Digital Publishing, Shih Hsin University, Taiwan, R.O.C.

characterization processes. To avoid both unpleasant discontinuity and swap rendition effects of lightness due to some unpredictable prediction error from model derived, a fuzzy k-cmeans clustering operation on lightness for color image segmentation will also be integrated in this work. This algorithm is used to enhance transition smoothness on color-appearance of rendered images. Preliminarily a color difference formula of CIE2000 (i.e. ΔE^*_{00}) will be adopted to investigate models' performance by using the training sets, which also establish the color gamut of imaging device considered.

Secondarily, a halftone-palate type of image display model, forhigh-fidelity soft-proofing and facsimile simulation of 6- or 7-colorants printing system, is also derived in this study. An Adobe RGB format of wide-gamut LCD display and a retina type of MacBook Pro are tested for this work. Mainly, three general classes of contone-to-halftone conversion process will be implemented and evaluated in this work. These are: 1) point-to-point process: including cluster, recursive and dispersed template; 2) chunk-to-point process: including iterative and error diffusion; 3) Hybrid point and chunk. All processes involve an iterative thresholding operation using CIEDE2000 color-difference formula, for the "find closest color", to match the input color to the closest available hardware color palette from 32 (i.e. 25) and 64 (i.e. 26) combinations, applied in the simulation of 5- and 6- colorants printing systems respectively.

The color difference formula of CIEDE2000, via the investigation of the correspondent training set, were also adopted here to optimize the prediction and rendition performances for both halftone-conversion of printing and display processes. Efforts will be also made on advanced development, modifications and integration of previous derived works, including the three-band CCD camera module (for multispectral measurement and/or reconstruction), an Adobe RGB format of wide-gamut LCD display and a retina type of MacBook Pro, a high-definition multicolor printing process (6/7 colorants, i.e. CMYKOG, CMYKRGB), tone/gamut mapping and color appearance model, and the halftone method derived.

Both of complex and computer-graphic HDR color images will be used in an advanced evaluation of models performance by adopting a forced-choice paired-comparison experiment. Therefore, via the bridge of these two well-performed modules derived in this research, hopefully, an optimized cross-media HDR contone-to-halftone Hi-Fi color transform module on both hardcopy and softcopy will be successfully proposed to form a complete color reproduction pipeline, and used as a main workflow in the process of color management.

Introduction

As desktop color publishing systems become more ubiquitous, the technical community, therefore, is being driven by the high-end color market to develop new technologies of HDR imaging and Hi-Fi color printing process, to differentiate and add value to their product. The intent is, via the use of HDR contone image, to produce Hi-Fi halftone images which have superior color with maximum isomerism, an increase of the attainable color gamut, and more tone and detail than those with traditional processes.

Additionally, in the field of Graphic Arts, multiple-primary displays with high-definition or wide color-gamut are practically used as soft-proofing for desktop color publishing. Therefore, as motivated by the idea to bridge the gap between high-dynamic-range (HDR) imaging and high-fidelity color reproduction in the high-end of Graphic Arts industry, the aim of this research has two tasks. Firstly, it's to derive an HDR contone to Hi-Fi halftone-conversion characterization model for both six-colorant CMYKOG and seven-ink CMYKORG printing systems, via fitting spectral-reflectance approach. It is optimally revised and extended from a previous research [1-3]. The supersets of CMYKOG and CMYKRGB were divided into three subsets and four subsets respectively. The superset of CMYKOG consisted of two five-colorant subsets of CMYKO and CMYKG, and one four-colorant subset of CMYK; whereas the CMYKRGB applies three five-colorant subsets of CMYKR, CMYKG and CMYKB, and one four-colorant subset of CMYK. The spectral printing characterization carries out a polynomial regression approach with singular value decomposition method (SVD). In total, 1617 and 1716 color patches were respectively used in test targets of four-colorant and five-colorant subsets for the printing characterization processes. Preliminarily a color difference formula of CIEDE2000 (i.e. ΔE^*_{00}) was adopted to investigate models' performance by using the training sets, which were also used to establish the color gamut of imaging device considered.

Further efforts was also made on advanced development, modifications and integration of the previous derived works, including a simulated three-band CCD camera module (for multispectral measurement and/or reconstruction), an Adobe RGB format of wide-gamut LCD display, high-definition multi-color printing processes (6/7 colorants, i.e. CMYKOG, CMYKRGB), tone/gamut mapping [4], and the halftone dithering method derived here.

The work below describes the experimental design used to firstly carry out the characterization of Hi-Fi printing devices, then followed by the derivation of an ideal CIEXYZ camera model, and finally the development of a halftone-palate type of image display model, for high-fidelity soft-proofing of 7-ink or 6- colorant printing system.

Experimental Procedure

Hi-Fi Printing Device Characterization

In practice, multi-color separation of 5-8 colors is used for Hi-Fi color printing systems. Summarily, two main ideas have been enduringly suggested and induced for the use of Hi-Fi processes. These are: 1) to optimize the smoothness of image detail from highlight to shadow; 2) to compensate for the gamut of secondary colors. The former idea is mostly adopted for the enhancement of imaging details by using the same hues but different concentrations from those of standard CMY inks (e.g. CMYKLcLm). As for the later one, it's for the extension of printability gamut with quite different hues from C, M, and Y colors (e.g., CMYKRGB, or CMYKOG as studied in this work).

Dominant Ink	Subgamut	Key Component
Black	CMYK	Black
Red	CMYKR	Red
Green	CMYKG	Green
Blue	CMYKB	Blue

Table 1: *Four subsets of 7-ink color separation.*

Dominant Ink	Subgamut	Key Component
Black	CMYK	Black
Orange	CMYKO	Orange
Green	CMYKG	Green

Table 2: *Three subsets of 6-colorant color separation.*

The printing characterization model in this paper was extended and further optimally modified from previous works [1-4] as mentioned earlier. These works were independently categorized into two different researches, which multi-spectrally modeled two printing processes of a heptatonic CMYKRGB press and a hexatonic CMYKOG printer respectively. However, the approach applied in these two multi-colorant models was mainly based on 5-colorant set, instead of 4-ink set which was original scheme suggested by Boll [5]. In the work of CMYKRGB color-separation, as shown in Table 1, the superset of 7-ink was subdivided into 4 subsets, including three 5-ink groupings of CMYKR, CMYKG and CMYKB, and one 4-ink grouping of CMYK. The 4-ink subset of CMYK abides by ANSI IT8.7/4 target, having 1,617 color patches. As for the test target used for every 5-ink subset, 1716 colors patches were contained. Both the dominant inks and the key- (extra-) components are black, red, green, and blue for CMYK, CMYKR, CMYKG, and CMYKB respectively. A Heidelberg CX 102-4 press was used. Similarly, as shown in Table 2, the same subdivision approach and concept used for the previous CMYKRGB system was also applied in the CMYKOG superset for a proofer, Epson Stylus Pro 9900 printer.

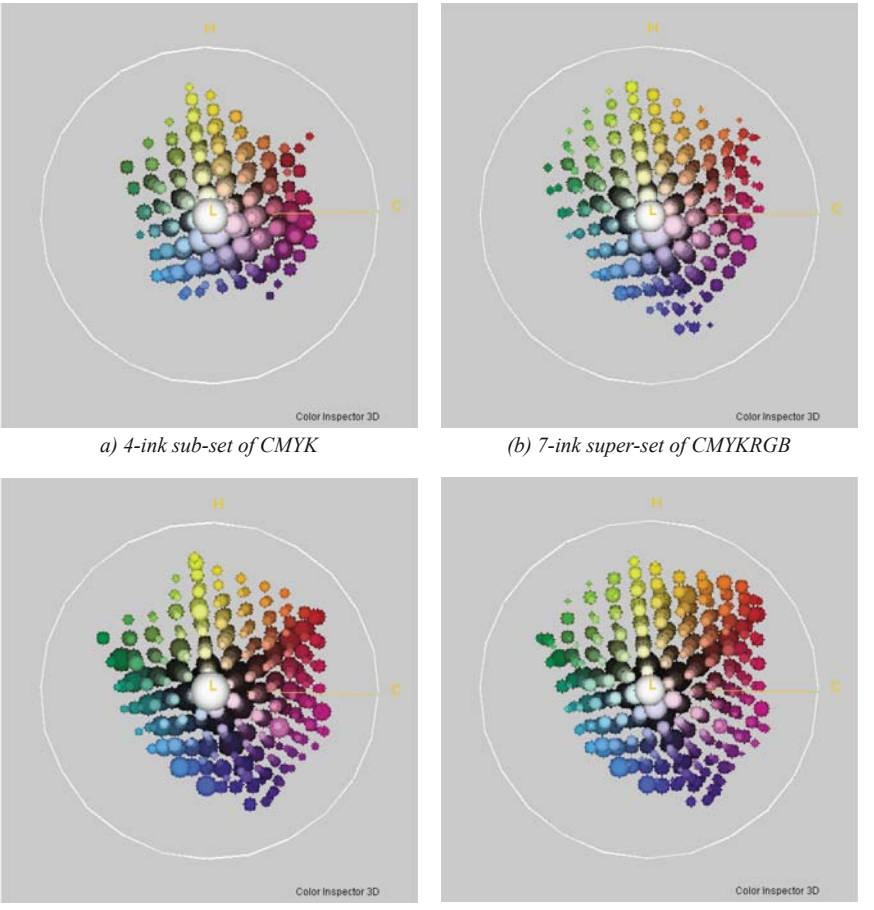

a) 4-ink sub-set of CMYK *(b) 7-ink super-set of CMYKRGB*

(c) 4-colorant sub-set of CMYK *(d) 6-colornat super-set of CMYKOG*

Figure 1: *Illustration of the extension of color gamut produced by using Hi-Fi of CMYKRGB inks [(a) compared to (b)] and CMYKOG colorants [(c) compared to (d)].*

As shown in Figure 1, the use of Hi-Fi of CMYKRGB inks (shown in (a)) could extend the color gamut, apparently regions of mainly secondary colors of red, green and blue, beyond what can be achieved in the conventional CMYK printing system (b); whereas the use of Hi-Fi of CMYKOG colorants (shown in (c)) expands regions of orange to green compared to those of the CMYK (d).

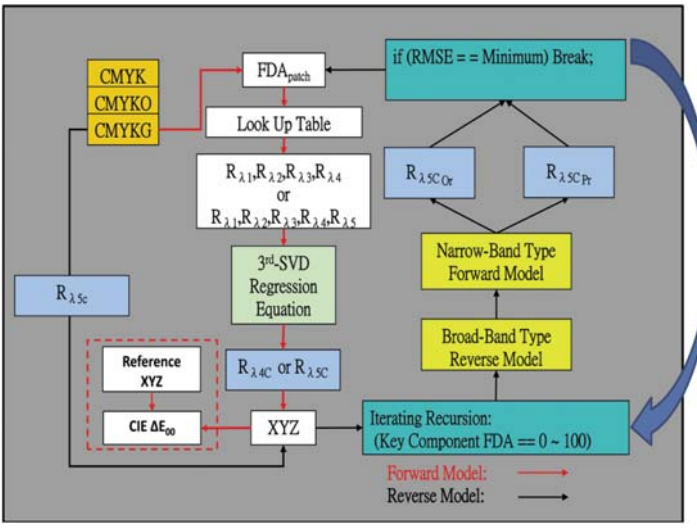

Figure 2: *Computational procedure for the characterization of 6-colorant proofer using multispectral approach for both processes of a forward and a reverse.*

The computational procedures in this study for Hi-Fi printing characterization of 6-colornat and 7-inks were similar. The superset of CMYKOG was initially divided into three subsets as mentioned above. The characterization of each subset was separately carried out using the masking-type model. It defines the transform between device-independent colorimetric/spectral data and device- dependent colorant data in its own corresponding sub-gamut of color space. All the printing models applied here were incorporated with the singular-value decomposition (SVD) method [6]. Figure 2 illustrates the whole picture of computation procedures for CMYKOG characterization model. In this diagram, the left side shows the forward process, and the right side for the reverse. In the forward process, for every subset, the FDAs of every color patch of interest in test target was firstly input into LUT to obtain the spectral data, corresponding to every colorant in the subset. Then, via the 3rd-order model, the spectral values, and also XYZ data of overprint would be predicted. Therefore, the prediction performance of forward model could be further analyzed using CIEDE2000. As for the reverse model, the original XYZ values of color patch in question, with a known iterative key-component FDA, was firstly input into the reverse process of broadband type and then multispectral type. Subsequently, with an optimization recursion process using RMSE and color difference, the spectral data and final colorants' FDAs of overprint would be predicted.

Approaches of both broadband (BB) and multispectral narrowband (MB), integrated in the experimental design, explored in the characterization both tested printing devices. Numerically both MB and BB models applied a 3rd-order and a 2nd-order with 3rd-order polynomial regression equations, respectively (as shown in Tables 3 to 5). Here the 'E' denotes Extra (i.e. Key) colorant used in each of 5-colornat/5-ink

subsets (e.g. CMYKE is CMYKO if the subset of interest is CMYKO). Each of BB and MB models carried out both processes of a forward and a reverse transform. The forward maps the device-dependent data (including spectral reflectance (SR) and fractional dot areas (FADs), of a color in question to its device-independent values (i.e. CIEXYZ, CIELAB, or CIELCh); while the reverse transforms device-independent values into device- dependent data (i.e. SR/FDAs). The broadband type of 2nd-SVD model (referred as 2nd-SVD-BB later) was derived from previous works as mentioned. Essentially, with a little detailed depth of study in those Tables 3 to 5, it could be seen that the concept applied for multispectral model is similar to those of the broadband. It just uses spectral reflectance data instead of colorimetric densities.

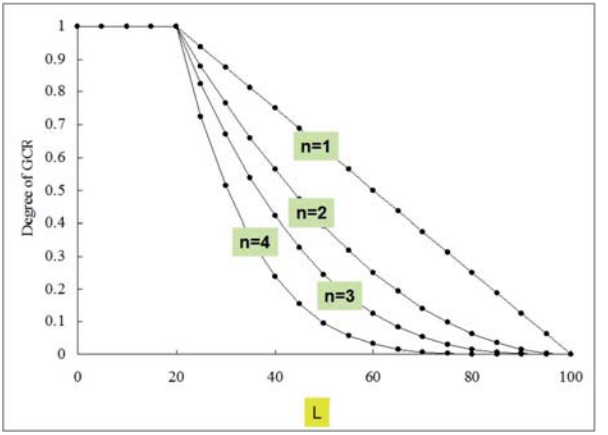

Figure 3: *Adaptive Type of GCR➞ ß = [(100-L*)/80]^n*

In this work, as conventional practice, the printer model derived also incorporated with an adaptive type of the GCR algorithm in the process of CMYK subset. As shown in Figure 3, the higher the n value, the higher degree of GCR used for shadow areas and the lower degree of GCR for highlight areas in the reproduction process.

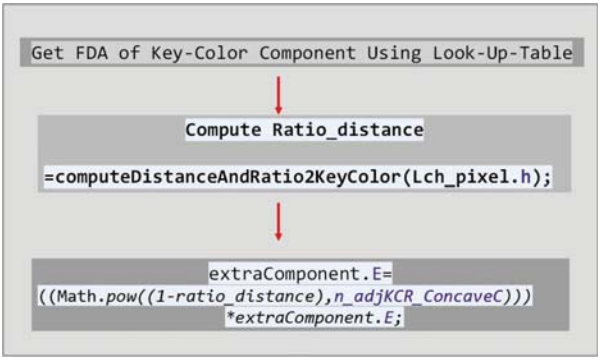

Figure 4: *Computational procedure for KCR algorithm derived.*

order	Parameters	No. of Term	Polynomial Regression Model
n^{order}-SVD Equation	m	$(\sum_{i=0}^{n} H_i^m)+1$	$\sum_{j=1}^{C_n^{m+n-1}} a_j n^{Order}(m) + \sum_{j=C_n^{m+n-1}+\ldots+1}^{C_n^{m+n-1}+C_{n-1}^{m+n-2}\ldots\ldots} a_j (n-1)^{Order}(m) + \ldots + 1$
3rd-SVD Equation (MB)	$R_{\lambda C}$ $R_{\lambda M}$ $R_{\lambda Y}$ $R_{\lambda K}$ $R_{\lambda E}$	$(\sum_{i=0}^{3} H_i^5)+1$ $=56$	$\sum_{j=1}^{C_5^3} a_j 3^{rd}(R_{\lambda C}, R_{\lambda M}, R_{\lambda Y}, R_{\lambda K}, R_{\lambda E}) + \sum_{j=C_5^3+1}^{C_5^3+C_5^2} a_j 2^{nd}(R_{\lambda C}, R_{\lambda M}, R_{\lambda Y}, R_{\lambda K}, R_{\lambda E}) + \sum_{j=C_5^3+C_5^2+1}^{C_5^3+C_5^2+C_5^1} a_j 1^{st}(R_{\lambda C}, R_{\lambda M}, R_{\lambda Y}, R_{\lambda K}, R_{\lambda E}) + 1$
2nd-SVD Equation (BB)	D_{r4C} D_{rE} D_{g4C} D_{gE} D_{b4C} D_{bE}	$(\sum_{i=0}^{2} H_i^6)+1$ $=28$	$\sum_{j=1}^{C_6^2} a_j 2^{nd}(D_{r4C}, D_{g4C}, D_{b4C}, D_{rE}, D_{gE}, D_{bE}) + \sum_{j=C_6^2+1}^{C_6^2+C_6^1} a_j 1^{st}(D_{r4C}, D_{g4C}, D_{b4C}, D_{rE}, D_{gE}, D_{bE}) + 1$

Table 3: *Polynomial models using SVD method in CMYKE process.*

2nd-SVD Equation (BB)	D_{r3C} D_{rBlack} D_{g3C} D_{gBlack} D_{b3C} D_{bBlack}	$(\sum_{i=0}^{2} H_i^6)+1$ $=28$	$\sum_{j=1}^{C_5^2} a_j 2^{nd}(D_{r3C}, D_{g3C}, D_{b3C}, D_{rBlack}, D_{gBlack}, D_{bBlack}) + \sum_{j=C_5^2+1}^{C_5^2+C_5^1} a_j 1^{st}(D_{r3C}, D_{g3C}, D_{b3C}, D_{rBlack}, D_{gBlack}, D_{bBlack}) + 1$
3rd-SVD Equation (MB)	$R_{\lambda 1}$ $R_{\lambda 2}$ $R_{\lambda 3}$ $R_{\lambda 4}$	$(\sum_{i=0}^{3} H_i^4)+1$ $=35$	$\sum_{j=1}^{C_4^3} a_j 3^{rd}(R_{\lambda 1}, R_{\lambda 2}, R_{\lambda 3}, R_{\lambda 4}) + \sum_{j=C_4^3+1}^{C_4^3+C_4^2} a_j 2^{nd}(R_{\lambda 1}, R_{\lambda 2}, R_{\lambda 3}, R_{\lambda 4}) + \sum_{j=C_4^3+C_4^2+1}^{C_4^3+C_4^2+C_4^1} a_j 1^{st}(R_{\lambda 1}, R_{\lambda 2}, R_{\lambda 3}, R_{\lambda 4}) + 1$

Table 4: *Polynomial models using SVD method in CMYK process.*

3rd-SVD Equation (BB)	D_{rc} D_{gm} D_{by}	$(\sum_{i=0}^{3} H_i^9)+1$ $=20$	$\sum_{j=1}^{C_3^3} a_j 3^{rd}(D_{rc}, D_{gm}, D_{by}) + \sum_{j=C_3^3+1}^{C_3^3+C_3^2} a_j 2^{nd}(D_{rc}, D_{gm}, D_{by}) + \sum_{j=C_3^3+C_3^2+1}^{C_3^3+C_3^2+C_3^1} a_j 1^{st}(D_{rc}, D_{gm}, D_{by}) + 1$ $\sum_{j=1}^{10} a_j 3^{rd}(D_{rc}, D_{gm}, D_{by}) + \sum_{j=10+1}^{10+6} a_j 2^{nd}(D_{rc}, D_{gm}, D_{by}) + \sum_{j=10+6+1}^{10+6+3} a_j 1^{st}(D_{rc}, D_{gm}, D_{by}) + 1$ 3^{rd}: $(a_1 D_{rc}^3 + a_2 D_{gm}^3 + a_3 D_{by}^3 + a_4 D_{rc}^2 D_{gm} + a_5 D_{rc}^2 D_{by} + a_6 D_{gm}^2 D_{rc} + a_7 D_{gm}^2 D_{by} + a_8 D_{by}^2 D_{rc} + a_9 D_{by}^2 D_{gm} + a_{10} D_{rc} D_{gm} D_{by})$ 2^{nd}: $(a_{11} D_{rc}^2 + a_{12} D_{gm}^2 + a_{13} D_{by}^2 + a_{14} D_{rc} D_{gm} + a_{15} D_{rc} D_{by} + a_{16} D_{gm} D_{by})$ 1^{st}: $(a_{17} D_{rc} + a_{18} D_{gm} + a_{19} D_{by} + a_{20})$

Table 5: *Polynomial models using SVD method in CMY process.*

As for the color involving extra- or key- inks or colorants, an adaptive KCR algorithm was revised from GCR in theory. It was applied in the 3rd-SVD-MS model used for every 5- colorant/ink. Here, a simple flow chart of calculation procedure (Figure 4) is given to demo a slight concept of how KCR was implemented since it is a little bit complicated. In the iteratively recursive process of adaptive optimization, the FDA of total key-color component for every pixel considered was obtained via LUT. Subsequently, via the computation of the hue-distance and the proportion (i.e. ratio) of the pixel considered to solid key-color-patch, the amount of extra- or key- component used would be calculated. Then, the actual FDA of key- colorant/ink for every 5-C subset could be predicted. Again, the prediction process would be iteratively optimized in terms of CIEDE2000 color difference. The function used for the calculation of the amount of extra- or key- component (i.e. "extraComponent.E" in Figure 4) is conceptually similar to the one introduced for the adaptive of GCR shown in Figure 3.

Subset	CMYK		CMYKR		CMYKG		CMYKB	
Process	F	R	F	R	F	R	F	R
Max	5.27	4.85	5.33	5.34	4.89	4.97	6.47	4.94
Average	1.15	0.92	1.26	1.85	0.99	1.67	1.00	1.61
ΔE_{00} >6 Count	0	0	0	0	0	0	1	0
RMSE (Mean)	0.0013	0.0018	0.0011	0.0028	0.0011	0.0027	9.78 E-4	0.0026

Table 6: *Summary of Prediction performances of the multi-spectral 2nd-SVD model (CMYKRGB).*

The prediction performances of derived Hi-Fi printer model were evaluated in terms of measures of Average (i.e. mean E00) Max (i.e. maximum E00), "ΔE_{00} >6 Count", and mean RMSE (root mean square error) tested using every corresponding test targets (E_{00} is color difference of CIEDE2000). The E_{00}, color difference of CIEDE2000, was calculated between XYZ values of the predicted color-patch and those of the original target color-patch in question. The results obtained for the 6C CMYKOG model were similar to previous ones. Therefore, Table 6 summarizes only the prediction performance of derived Hi-Fi 7-C CMYKRGB printing model proposed using each of 4- and 5-colorant subsets. Every subset was performed both forward (F) and reverse (R) transforms. It showed, as seen from the Average ΔE_{00}: the 7-ink characterization model overall performed significantly satisfactory predictions.

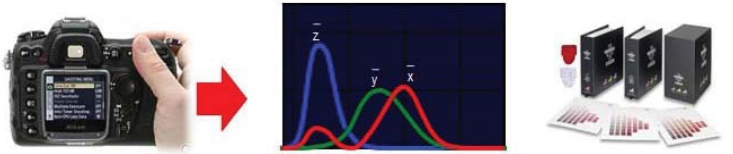

Figure 5: *The development of idea CIEXYZ camera model using the spectral color dataset of Munsell Book Glossy.*

Multispectral CIEXYZ Sensing Model

As mentioned, this work also applied multispectral approach for both Hi-Fi printing systems. It was, hence, needed to carry out a multispectral type of input device model to obtain multispectral type of input image data. Therefore, a well- performed multispectral type of camera sensing model, derived in a previous research [1] was also designed in this work. This spectral sensing model was virtually equipped with the simulated CIEXYZ three-band filters, i.e. CIE 1931 color matching functions. The development of Ideal CIEXYZ camera in this research used an appropriate real spectral color dataset of Munsell Book Glossy [6] as shown in Figure 5. Also, both the SVD and the Winner-inverse methods were integrated and employed here as an estimator to minimize MSE (Mean Square Error) of the spectral radiance of every pixel between the original and the predicted images. It was characterized under the standard illuminant D50.

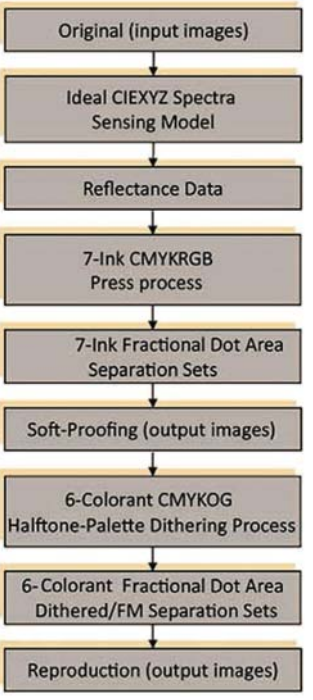

Figure 6: *Processes of both FM and halftone-palette half-toning/dithering.*

Halftone-Palette Dithering

As for the work of halftone palette on both soft-proofing and hard-proofing applications, four dithering methods were implemented in this work. This work was originally stimulated by a web-site [7] which is the implementation of Floyd-Steinberg dithering method. These four algorithms derived included (1) Floyd-Steinberg; (2) Jarvis, Judice and Linke; (3) Stucki; and (4) Alkinson dithering [8]. They were based on the concept of error diffusion to find the nearest palette color, chosen to the current pixel in question. Figure 6 demonstrates both processes of FM

(Frequency Modulation) and halftone- palette half-toning/dithering to transform the original HDR images, via the ideal spectral sensing and both 7-ink and 6-colorant printing separation models, to 6- colorant of hardcopy and softcopy proofing respectively.

Of course, there are many ways to find the nearest palette color (with varying levels of efficiency and quality). As described in the website just mentioned, it uses a trivial algorithm that finds the nearest palette color with minimum straight-line distance in the RGB color cube from the given color. However, to improve levels of efficiency and quality, in our approach, the minimum of color difference of CIEDE2000 (i.e. E00) was used instead of the difference of RGB. Therefore, with a little further of calculation, then, 128 and 64 color palettes were obtained and used as the index schema of LUT for CMYKRGB and CMYKOG processes respectively.

Results and Discussion

Figures 7 to 8 demoes the Hi-Fi color-fidelity rendition results, rendered from both 7-ink and 6-colorant printing characterization modules tested. Finally, Figure 9 gives one set of simulated dithered soft-proofing results using 6- colorant halftone-palette type of image data. The obtained results, with close evaluations, significantly showed that both multispectral types of Hi-Fi printing models all efficiently well-performed. From those rendered results, it was also apparently revealed that the whole CMS chain of Hi-Fi cross-media color reproduction derived in this research could satisfactorily reproduce pleasing representations of original-referred HDR images displayed in Adobe format of LCD.

(a) Final rendition results using both processes of 4-ink (top) and 7-ink (bottom) models.

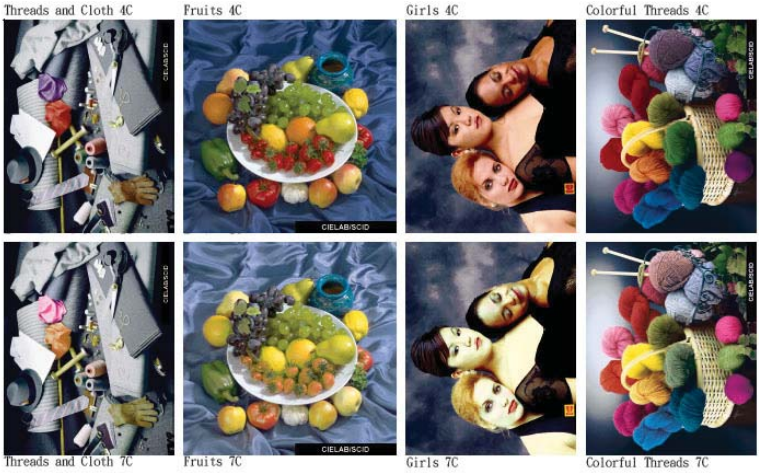

(b) Partial rendition results using both 4-ink (top) in 4C subset and 4-ink out of 7C superset (bottom).

(c) Partial rendition results using 3-ink of RGB (bottom), out of 7-ink superset.

Figure 7: *Rendition results using 7-ink printing model.*

The CMS system derived could carry out properly optimal iterations of the combination of both adaptive KCR and GCR algorithms, with the well- performing plugged CIEXYZ image-sensing camera model and halftone-palette dithering techniques.

(a) Final rendition results using both processes of 4-colorant (top) and 6- colorant (bottom) models

(b) Partial rendition results using both 4-colorant (top) in 4C subset and 4- colorant out of 6C superset (bottom)

(c) Partial rendition results using 2-colorant of OG (bottom), out of 6-colorant superset.

Figure 8: *Rendition results using 6-colorant printing model.*

Figure 9: *Halftone-palette dithering results using 6-colorant printing model.*

Conslusions

As inspired by the idea to link the connection between high-dynamic-range (HDR) imaging and high-fidelity color reproduction in the high-end of Graphic Arts industry, this research had resonantly fulfilled two tasks. They were optimally revised and extended from previous research works:

Firstly, the derivation of characterization models, processing the conversion of image data between HDR contone and Hi-Fi halftone formats, via fitting spectral-reflectance approach. Then, by doing this, we could produce:

(a) Hi-Fi halftone images of superior color with maximum retraining from the isomerism phenomenon;

(b) An increase of the attainable color gamut; and

(c) More tones and details than those with traditional processes.

Additionally, in the field of Graphic Arts, multiple-primary displays with high-definition or wide color-gamut are practically used as soft-proofing for desktop color publishing. Various halftone-palate type of image display models were, hence, satisfactorily introduced and adopted for soft-proofing and simulation of high-fidelity (7-ink or 6-colorants) printing systems.

References

1. Lo, M. C., Lin, J. L., Guo, C. Z., and Ma, H. K., "Robust spectral implementation of high-fidelity printer characterization for cross-media high-dynamic-range imaging application", NIP (Digital Printing Technologies) and Digital Fabrication 2011, pgs. 29-33, 2011 (ISBN / ISSN: 978-89208-296-4).
2. Lo, M. C., Chen, C. L., and Hsieh, T. H., "Characterization of high- fidelity color printing devices based on both multispectral and broadband approaches", The 9th International Symposium on Multispectral Colour Science and Application, pgs. 36-44, May 2007.
3. Lo, M.C., Chen, C.L., and Hsieh, T.H., "Characterization of high-fidelity color printing devices using illuminant-independent approaches for color imaging application", NIP 24: 24th International Conference on Digital Printing Technologies, pgs. 597-602, 2008.
4. Lo, M. C., Chen, H. S., and Chueh, C. P., "The design of advanced gamut mapping algorithms in color management systems", TAGA proceeding, pgs. 3-15, 2003.
5. Boll, H. "A color to colorant transformation for a seven ink process". IS&T's Third Technical Symposium on Prepress, Proofing, & Printing, 3, pgs. 31-36,1993.
6. Orava, J., The reflectance spectra of 1600 Glossy Munsell Color Chips. (http://spectral.joensuu.fi/databases/download/munsell_spec_glossy_all.htm)
7. http://en.literateprograms.org/Floyd-Steinberg_dithering_(Java)
8. Wong, P. W., "Adaptive error diffusion and its application in multiresolution rendering," IEEE Tran. Image Processing, vol. 5, pgs. 1184-1196, July 1996.

Acknowledgements

The authors would like to acknowledge the following company for their help in the project: SHEN'S ART PRINTING Co., LTD. The authors would also like to acknowledge the National Science Council of Taiwan for financial assistance in this research work.